pISSN 1229-3008 eISSN 2287-6251
Progress in Superconductivity and Cryogenics
Vol.18, No.1, (2016), pp.55~58
http://dx.doi.org/10.9714/psac.2016.18.1.055

Study on quench detection of the KSTAR CS coil with CDA+MIK compensation of inductive voltages

Seok Chan An[a,b], Jinsub Kim[a,b], Tae Kuk Ko[a], and Yong Chu[*,b]

[a]*Yonsei University, Seoul, Korea*
[b]*National Fusion Research Institute(NFRI), Daejeon, Rep. of Korea*

(Received 13 February 2016; revised or reviewed 24 March 2016; accepted 25 March 2016)

Abstract

Quench Detection System (QDS) is essential to guarantee the stable operation of the Korea Superconducting Tokamak Advanced Research (KSTAR) Poloidal Field (PF) magnet system because the stored energy in the magnet system is very large. For the fast response, voltage-based QDS has been used. Co-wound voltage sensors and balanced bridge circuits were applied to eliminate the inductive voltages generated during the plasma operation. However, as the inductive voltages are hundreds times higher than the quench detection voltage during the pulse-current operation, Central Difference Averaging (CDA) and MIK, where I and K stand for mutual coupling indexes of different circuits, which is an active cancellation of mutually generated voltages have been suggested and studied. In this paper, the CDA and MIK technique were applied to the KSTAR magnet for PF magnet quench detection. The calculated inductive voltages from the MIK and measured voltages from the CDA circuits were compared to eliminate the inductive voltages at result signals.

Keywords: Quench Detection System, KSTAR, Central Difference Averaging, MIK

1. INTRODUCTION

For large scale coils, such as Korea Superconducting Tokamak Advanced Research (KSTAR) coils, the role of the Quench Detection System (QDS) is essential because large energy is stored in the coils. Voltage based QDS has been used for the fast detection to limit the temperature rise and avoid the conductor degradation. As inductive voltages can be obstacles for the reliable quench detection, various techniques have been used to compensate the inductive voltages generated by pulse-current operation [1], [4]. Reducing the inductive voltage terms is necessary because the inductive voltage level can be much higher than the resistive voltage level caused by quench. Ideally, whole inductive voltage terms should be excluded to detect resistive voltage promptly.

Particularly, the fusion magnet system in KSTAR or ITER consists of many coils, where Central Solenoid (CS) and Poloidal Field (PF) coils operate in pulse current. The inductive voltages reach a few kV in KSTAR and tens of kV in ITER, which can be generated by self- and mutual inductances.

For the multiple coil system, bridge circuits are not effective to eliminate inductive voltages. Co-wound voltages sensors, which are wounded in the same winding direction, have good inductive voltage compensation, but disassembly of magnet system is in need to repair when they are impaired.

Central Difference Averaging (CDA) was suggested for the reduction of inductive voltages. Unlike bridge circuits, CDA circuits do not use potentiometers. The compensation of the inductive voltage is achieved by subtracting the average of the first and the third coil winding voltages from the second coil winding voltage.

Mutual inductance compensation or MIK, where I and K stand for mutual coupling indexes of different circuits [2], can be implemented by using microprocessor as a technique to actively compensate the inductive voltage by taking mutual inductances between coils into account. In this paper, the CDA combined with MIK technique was applied to the KSTAR magnet for the quench detection of PF1 coil to verify the effectiveness of the method.

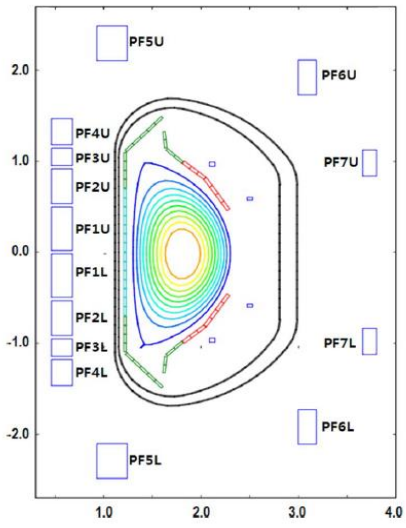

Fig. 1. Geometry of the KSTAR PF magnet system, which includes CS Coils (PF1-4) and PF coils (PF5-7) [3].

* Corresponding author: ych@nfri.re.kr

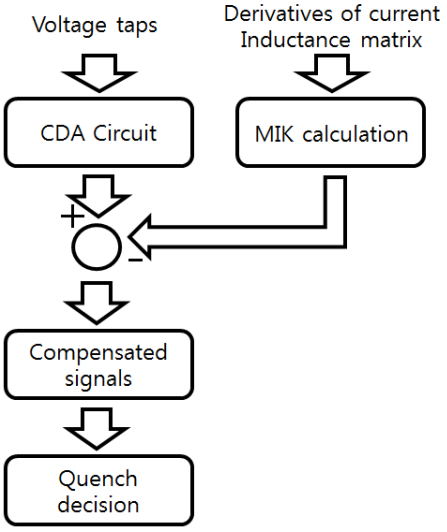

Fig. 2. The basic methodology to implement the CDA combined with MIK on KSTAR PF coils.

2. CDA AND MIK

2.1. Basics

The KSTAR PF magnet system consists of 14 coils with 11 different power supplies, which supply different currents at the same time.

The PF coils are vertically symmetric to the mid-plane as shown in Fig. 1. Except PF6U and PF6L, the other PF coils have three voltages taps at both the end terminals and the center of each coil, from which voltages of a half of each coil can be addressed. For the PF6U and PF6L coils, five voltage taps in each coil can measure voltages of a fourth of each coil.

As shown in Fig. 2, the CDA signals are achieved from CDA circuit voltage taps and MIK signals are calculated from the derivative of current and inductance. Quench decision is made by combination of both signals.

2.2. Simple CDA

In this paper, CDA circuit is applied to the first, second and third coil windings of the PF 1 coil, where PF1U and PF1L are series-connected. The fundamental concept of simple CDA is shown at Eq. (1). The average of the first and the third coil winding voltage is subtracted from the first coil winding voltage. Thus, the coefficient for the simple CDA is 0.5. Each V1, V2 and V3 in Eq. (1) includes the summation of mutually inductive voltage by the other PF coil windings, eddy currents on structures and plasma current. According to the Eq. (1), most of the self and mutual inductance terms can be eliminated. However, measured CDA signal is not a zero signal mostly due to un-canceled self and mutual inductance terms.

$$\begin{aligned} V_{CDA1} &= V_2 - 0.5(V_1 + V_3) \\ &= \{L_2 - 0.5(L_1 + L_3)\}\frac{di}{dt} + \{M_{13} + M_{32} + M_{42} \\ &-0.5(M_{21} + M_{31} + M_{41} + M_{13} + M_{23} + M_{43})\}\frac{di}{dt} \quad (1) \end{aligned}$$

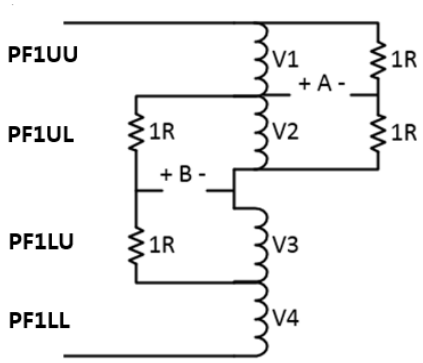

Fig. 3. 1R type CDA circuit for PF 1 coil.

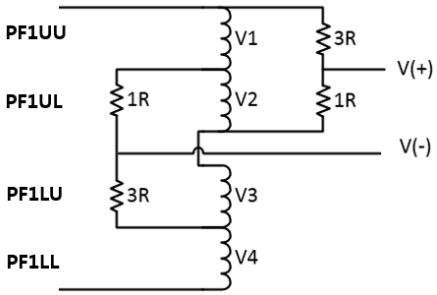

Fig. 4. 3R type CDA circuit for PF 1 coil.

2.3. 1R type CDA circuit

The 1R type CDA circuit uses voltage bridges with two pairs of 1:1 ratio voltage divider. As described in Eq. (2), the CDA signal can be achieved from the summation of voltage bridge signals, A and B. The final signal can be achieved by the first digital signal summation.

$$A = \frac{1}{2}(V_{L2} - V_{L1})$$

$$B = \frac{1}{2}(V_{L2} - V_{L3})$$

$$A + B = \frac{1}{2}(V_{L2} - \frac{V_{L1} + V_{L3}}{2}) \quad (2)$$

2.4. 3R type CDA circuit

The 3R type CDA circuit is shown in Fig. 4. It uses two voltage bridges with 3:1 and 1:3 ratio voltage dividers. As described in Eq. (3), the CDA signal can be achieved directly from the probe without extra digital signal processing.

According to the circuit equation, 1R type CDA circuit output and the two times of 3R type CDA circuit output has the same value. Thus, theoretically 1R type and 3R type CDA circuits will generate the same signal.

$$V_{(+)} = V_{L4} + \frac{3\mathrm{R}}{3\mathrm{R} + 1\mathrm{R}}(V_{L3} + V_{L2})$$

$$V_{(-)} = V_{L4} + V_{L3} + \frac{1\mathrm{R}}{3\mathrm{R} + 1\mathrm{R}}(V_{L1} + V_{L2})$$

$$V_{(+)} - V_{(-)} = V_{L2} - 0.5(V_{L2} + V_{L3}) \quad (3)$$

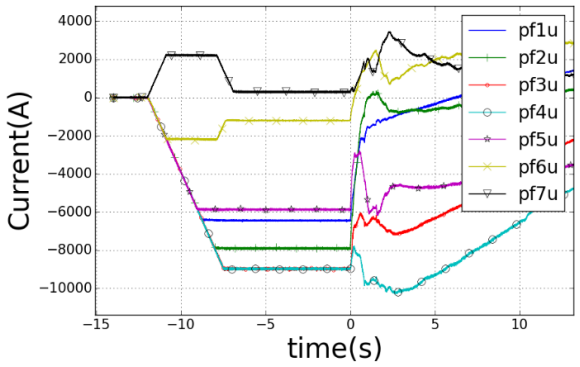

Fig. 5. The currents of 7 upper coil windings from 7 different power sources for shot #13697.

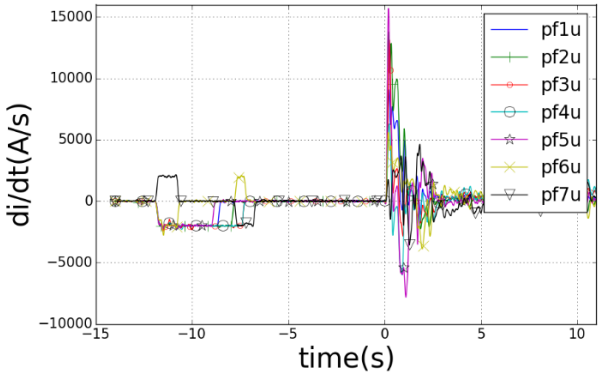

Fig. 6. The di/dt of 7 upper coil windings for shot #13697.

2.5. MIK calculation

The role of MIK is calculating the inductive voltage from current data and pre-calculated inductance matrix to compare with measured CDA voltage signals. MIK calculation result is expected to be very similar with the measured CDA voltage except for the noise and plasma current effect. Thus, MIK calculation was used to eliminate the remnant inductive voltage terms from CDA signals.

For the MIK, inductance matrix between PF1 coil and the other coils is in need. By a commercial FEM analysis tool, Infolytica MagNet, stored energies in the coil windings are calculated. Self and mutual inductances between windings were calculated from the relationship between stored energies and applied currents.

$$\begin{pmatrix} M_{11} & M_{12} & M_{13} & M_{14} & \cdots & M_{122} \\ M_{21} & M_{22} & M_{23} & & & \\ M_{31} & M_{32} & \cdot & & & \cdot \\ \cdot & & & \cdot & & \cdot \\ \cdot & & & & \cdot & \\ M_{221} & & & & & M_{2222} \end{pmatrix} \begin{pmatrix} di_1/dt \\ di_2/dt \\ \cdot \\ \cdot \\ \cdot \\ di_{22}/dt \end{pmatrix} = \begin{pmatrix} V_1 \\ V_2 \\ \cdot \\ \cdot \\ \cdot \\ V_{22} \end{pmatrix} \quad (4)$$

Temporal derivatives of PF currents were obtained by Rogowski coils. The inductive voltages of each PF coil windings were calculated by multiplying inductance matrix and di/dt matrix as shown in Eq. (4). Finally, V1, V2 and V3 were calculated according to the Eq. (1) to compare with the measured CDA signal [5, 6].

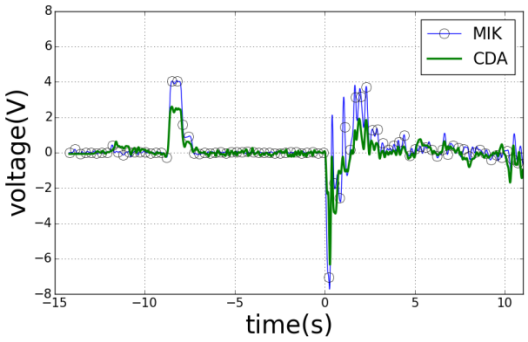

Fig. 7. 1R type CDA circuit signal and MIK signal for PF 1 coil at shot #13697.

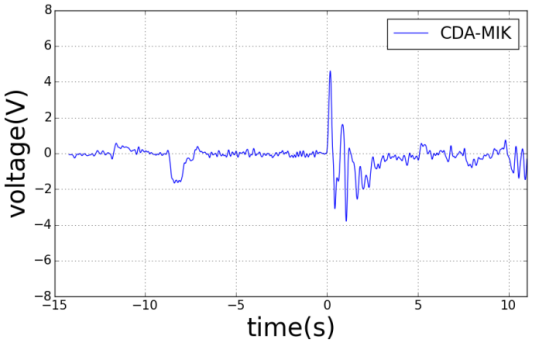

Fig. 8. 1R type CDA+MIK signal for PF 1 coil at shot #13697.

3. CDA+MIK RESULT

3.1. CDA+MIK (1R type)

The currents of 7 upper coil windings from 7 different power sources are shown at Fig. 5. The upper and lower coil windings of each PF1, PF2 and PF7 coil are connected in serial, thus the upper and lower coil windings have the same power source. The upper and lower coil windings of the PF 3 to 6 have their own power sources. After all, there exist 11 different current sources for the KSTAR PF magnet system.

Current data for the long-pulse plasma shot are shown at Fig. 5. Each coil is pre-charged to different level before t=0s. Then, current changes for the startup and the maintaining of plasma.

The 1R type CDA circuit was applied for shot #13697. As shown in Fig. 7, most of the inductive voltages were successfully compensated, so the resulting CDA signal levels are under 300mV. However, signals still rises up to 4V at t= -7s and -7.8V at t=2s because of the remnant inductance terms.

The similar trajectory of MIK signals with CDA signals proved that most of the CDA signal is caused by remnant inductive voltage. As shown in Fig. 7, MIK signals and CDA signals are similar even at minor fluctuation.

The combination of CDA and MIK was achieved by subtracting the CDA signal form the MIK signal. Most of the remnant inductive voltage terms are compensated. As shown in Fig. 8, the CDA+MIK signal level has reduced from 4 V to 1.7 V at=-7s and from -7.8V to -4.6V at t= 2s.

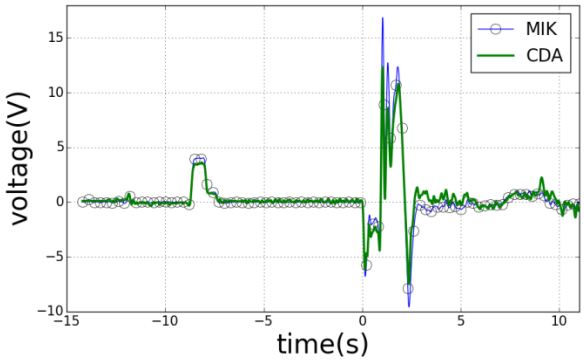

Fig. 9. 3R type CDA circuit signal and MIK signal for PF 1 coil at shot #14326.

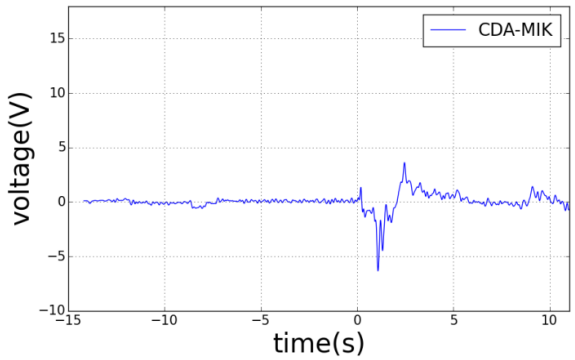

Fig. 10. 3R type CDA+MIK signal for PF 1 coil at shot #14326

3.2. MIK+CDA (3R type).

The 3R type CDA circuit was applied for shot #14326, which has similar property with shot #13697. As shown in Fig. 9, CDA signal levels rise up to 4V at t= -8.5s and 12V at t=1s. As shown in Fig. 10, the CDA+MIK signal level has reduced from 4V to 1.6V at=-8.5s and from 12V to 6.335V at t= 1s.

The combination of 3R type CDA and MIK calculation could lower the CDA+MIK signal levels by compensating the remnant inductive voltage.

4. CONCLUSION

The CDA circuit, both 1R type and 3R type could compensate most of the inductive voltages, but there still exist remnant inductance terms. MIK signals were calculated from inductance matrix and current data. The MIK signals were subtracted from CDA signals. As a result, most of the remnant inductive voltages in the CDA signals disappeared at the CDA+MIK signals over the shot. However, especially at the current ramping up and plasma startup phases, CDA+MIK signals are too high to distinguish resistive voltage from inductive voltages. The effect of plasma and eddy current is assumed to be one possible cause.

Research about Rogowski coils, digital signal processing and voltages induced by plasma and eddy currents on passive structures would be carried out for the CDA+MIK system.

ACKNOWLEDGMENT

This work was supported by the Korean Ministry of Science, ICT and Future Planning.

REFERENCES

[1] Y. Chu, H. Yonekawa, Y. O. Kim, K. R. Park, H. J. Lee, M. K. Park, Y. M. Park, S. J. Lee, T. H. Ha, Y. K. Oh, J. S. Bak, and K. Team, "Quench Detection Based on Voltage Measurement for the KSTAR Superconducting Coils," *IEEE Trans. Appl. Supercond.* vol. 19, no. 3, pp. 1565–1568, 2009.

[2] A.L. Radovinsky and J.H. Schultz, "Revised Blanking Model Of Baseline Scenario, Ending In Disruption, With Negative Mik, Combined With Optimized Alpha-Beta And Simple Central Difference Averaging," ITER-MIT-ALRadovinsky-071807-01, July 18, 2007

[3] Y. Chu, S. H. Park, H. Yonekawa, Y. O. Kim, H. J. Lee, K. P. Kim, S. J. Lee, K. R. Park, Y. K. Oh, and H. K. Na, "Quench Simulation and Detection in KSTAR PF Magnet System," *IEEE Trans. Appl. Supercond.*, vol. 20, no. 3, pp. 568–571, 2010.

[4] M. Coatanea-Gouachet, D. Carrillo, S. Lee, and F. Rodriguez-Mateos, "Electromagnetic Quench Detection in ITER Superconducting Magnet Systems," *IEEE Trans. Appl. Supercond.*, vol. 25, no. 3, pp. 1–7, 2015.

[5] H. T. Yeh, J. S. Goddard, and S. S. Shen, "Inductive Voltage Compensation In Superconducting Magnet System," *Proceedings of the 6th Symp. on Engr. Probl. of Fusion Research, IEEE*, pp. 1802, 1979.

[6] H. Yonekawa, Y. Chu, Y. Kim, S. Park, and K. Park, "Experimental Evaluation of a Mutually Inductive Voltage Correction Method to Improve the KSTAR Quench Detection System," *IEEE Trans. Appl. Supercond.*, vol. 23, no. 3, pp. 1–4, 2013.